JACS
JOURNAL OF THE AMERICAN CHEMICAL SOCIETY
Article
pubs.acs.org/JACS

Redox-Based Control of the Transformation and Activation of siRNA Complexes in Extracellular Environments Using Ferrocenyl Lipids

Burcu S. Aytar,[†] John P. E. Muller,[†] Yukishige Kondo,[§] Yeshayahu Talmon,*[,‡] Nicholas L. Abbott,*[,†] and David M. Lynn*[,†]

[†]Department of Chemical and Biological Engineering, University of Wisconsin—Madison, Madison, Wisconsin 53706, United States
[‡]Department of Chemical Engineering, Technion-Israel Institute of Technology, Haifa 32000, Israel
[§]Department of Industrial Chemistry, Tokyo University of Science, Shinjuku, Tokyo 162-8601, Japan

ABSTRACT: We report physical characterization and biological evaluation of complexes of small interfering RNA (siRNA) formed using a cationic lipid [bis(11-ferrocenylundecyl)dimethylammonium bromide (BFDMA)] containing redox-active ferrocenyl groups at the end of each hydrophobic tail. We demonstrate that control over the redox state of BFDMA can be used to influence key physical properties and control the activities of lipoplexes formed using siRNA-based constructs. Specifically, lipoplexes of siRNA and reduced BFDMA lead to high levels of sequence-specific gene silencing in cells, but lipoplexes formed using oxidized BFDMA do not. Lipoplexes of oxidized BFDMA can be activated *in situ* to induce high levels of silencing by addition of a chemical reducing agent, demonstrating a basis for external control over the activation/delivery of siRNA in cellular environments. Differences in activity arise from the inability of oxidized BFDMA to promote efficient internalization of siRNA; these differences also correlated to significant differences in the nanostructures of these lipoplexes (determined by cryo-TEM) and their ζ potentials as a function of oxidation state. These results are considered in view of recent studies characterizing the nanostructures, properties, and behaviors of lipoplexes formed using BFDMA and macromolecular plasmid DNA. We find that several key structural features and aspects of redox control observed for lipoplexes of plasmid DNA are maintained in complexes formed using smaller and more rigid siRNA. The ability to transform BFDMA in complex media presents opportunities to exert control over the nanostructures and behaviors of siRNA lipoplexes in ways not possible using conventional lipids. The approaches reported here could thus prove useful in both fundamental and applied contexts.

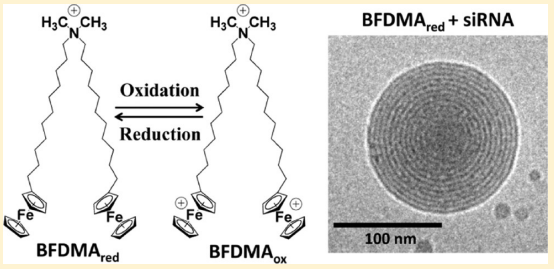

INTRODUCTION

RNA interference (RNAi) is a complex and evolutionarily conserved cellular process that results in the silencing of gene expression at the post-transcriptional level.[1−4] This process can be induced in mammalian cells using synthetic, double-stranded small interfering RNA (siRNA) sequences that promote the degradation of complementary mRNA and can therefore be used to knock down the expression of targeted genes in a highly specific manner.[1−7] For these and other reasons, RNAi has become a powerful tool for the investigation of fundamental cellular processes, and siRNA constructs are also now under intense investigation as potential therapeutic agents.[2−4,6−9] A more complete fundamental understanding of the processes underlying RNAi will continue to drive advances on both of these fronts. The successful translation of new knowledge arising from these basic studies into new therapeutic approaches, however, will also depend critically upon the development of methods and materials that provide new and useful levels of control over the transport of siRNA into cells.

Many different types of synthetic materials have been used to transport siRNA into cells.[4,7,10−17] Cationic lipids and lipid-like molecules, in particular, have been widely used to assemble nanoscale aggregates ("lipoplexes") that promote entry into cells and promote gene silencing *in vitro* and *in vivo*.[4,7,10,12,14−18] Because siRNA mediates the knockdown of targeted genes in the cytosol, and because many lipoplexes are internalized by endocytosis, much of the early and ongoing work in this area has focused on the development of lipids that promote endosomal escape and cytosolic delivery. These and other barriers to delivery have been addressed, in general, by either adopting materials and approaches originally developed for the delivery of plasmid DNA[7,10] or by developing new lipids or lipid-like materials (e.g., "lipidoids", etc.) designed specifically for use with siRNA.[19−22]

The first of these two approaches is attractive from both conceptual and practical points of view (e.g., existing cationic lipids designed to form electrostatic complexes with negatively charged DNA are also capable of doing so with siRNA). There are, however, many significant physicochemical differences between plasmid DNA and siRNA that can influence important biophysical properties of lipoplexes and impact their structures, behaviors, and biological activities.[15,17,19,23−25] Chief among these differences is size: whereas plasmid DNA is macro-

Received: April 9, 2013
Published: May 23, 2013

   dx.doi.org/10.1021/ja403546b | *J. Am. Chem. Soc.* 2013, 135, 9111−9120

molecular and often many thousands of bases long, siRNA is a short, rigid-rod oligomer of nucleic acids ~20 bases in length. Plasmid DNA can thus be physically compacted and condensed into nanoparticles upon complexation with cationic lipids; siRNA constructs also form nanoscale aggregates with cationic lipids but, by virtue of their small size and rigid character, they cannot be physically compacted in this way.[23,24]

Past studies have demonstrated that differences in size and related biophysical consequences (e.g., the greater mobility and additional degrees of translational/rotational freedom of siRNA relative to plasmid DNA) can lead to large differences in the structures and biological behaviors of siRNA- and DNA-based lipoplexes.[19,23−25] For example, X-ray diffraction studies of lipoplexes of siRNA formed using a mixture of the lipids DOTAP (1,2-dioleoyl-3-trimethylammoniumpropane) and DOPC (1,2-dioleoyl-*sn*-glycero-3-phosphatidylcholine) revealed lamellar nanostructures similar to those of plasmid DNA-based lipoplexes, but that siRNA-based lipoplexes exhibited higher degrees of local lipid ordering and that siRNA is present in these ordered phases in a state that is more isotropic and liquid-like than that observed in otherwise similar DNA-based lipoplexes.[24] That same study demonstrated that lipid:siRNA charge ratios required to achieve efficient gene silencing were an order of magnitude higher than those needed to promote high levels of transgene expression using plasmid DNA—an outcome that requires the use of substantially higher concentrations of lipid and attendant substantial increases in cytotoxicity in *in vitro* gene silencing experiments. Two other recent studies also reveal large differences in the nanostructures, biophysical properties, and biological behaviors of lipoplexes of siRNA and plasmid DNA formed using other cationic lipid systems.[19,25] As a result of the large physicochemical differences between plasmid DNA and siRNA, and owing to other substantial differences in both intracellular mechanisms and locations of action,[7,12,16] it is not generally possible to predict important functional properties of complexes of siRNA and cationic lipids solely on the basis of information gleaned from physical, biophysical, or biological studies of complexes formed using plasmid DNA.[19,23−25]

In view of the studies described above demonstrating differences in the structures and properties of lipoplexes formed using DNA and siRNA,[23,24] we sought to determine whether ferrocene-functionalized cationic lipids demonstrated previously to provide redox-based control over the structures and biological behaviors of lipoplexes of plasmid DNA could be used to transport siRNA into cells and promote the sequence-specific knockdown of targeted genes. Here, we report characterization and biological evaluation of nanoscopic siRNA lipoplexes formed using [bis(11-ferrocenylundecyl)-dimethylammonium bromide (BFDMA, Figure 1)], a cationic lipid containing redox-active ferrocenyl groups at the end of each hydrophobic tail.[26−28] Past studies demonstrated that BFDMA can be used to form lipoplexes that transport plasmid DNA to cells and promote high levels of reporter gene expression *in vitro* in a variety of cell types.[29−34] An important and unique finding arising from those past studies is that the oxidation state of the ferrocenyl groups in BFDMA (that is, whether they are present in the reduced or oxidized state; Figure 1) plays a critical role in determining whether lipoplexes are internalized by cells.[31,33] For example, whereas lipoplexes prepared using plasmid DNA and reduced BFDMA enter cells readily—and thereby promote high levels of transgene expression—lipoplexes prepared using oxidized BFDMA do not enter cells readily and thus promote much lower (negligible) levels of expression. Two recent studies demonstrated that the redox behavior of BFDMA can also be used to "activate" otherwise inactive lipoplexes of oxidized BFDMA, including in the presence of cells, by the controlled addition of chemical reducing agents (e.g., ascorbic acid[33] or glutathione[31]), suggesting the potential of the organometallic ferrocenyl functionality of this cationic lipid to provide opportunities to exert active, external, and *in situ* control over the biophysical properties and biological activities of these DNA-based complexes.

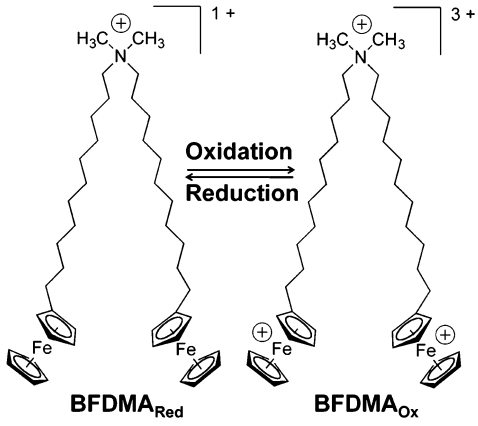

Figure 1. Structure of BFDMA.

The large differences in the activities of the DNA-based lipoplexes used in those past studies were found to correlate to significant differences in the nanostructures and the ζ potentials of the lipoplexes—two physical properties that depend strongly upon the nature of the interactions between reduced or oxidized BFDMA and plasmid DNA.[30,31,33−36] For example, whereas lipoplexes of DNA and reduced BFDMA have multilamellar nanostructures, inactive lipoplexes of DNA and oxidized BFDMA were found to be amorphous and have ζ potentials that were substantially more negative. The results of this current study demonstrate that this ferrocene-containing cationic lipid can be used to prepare lipoplexes of siRNA that promote effective gene silencing in cells and, significantly, that features of redox-specific "on/off" control of the biological activity observed using lipoplexes formed from plasmid DNA are largely preserved and maintained in lipoplexes formed using siRNA—without the need to further optimize lipid/siRNA charge ratios or change other aspects of nanoparticle formulation. The results of physicochemical characterization studies also reveal several key structural and biophysical features of these siRNA lipoplexes (e.g., differences in nanostructure, ζ potential, and mechanisms of cellular entry as a function of lipid oxidation state) to be similar to those observed in complexes of larger plasmid DNA. Our studies reveal, however, that the substantially smaller size of siRNA permits more extensive dynamic, nanoscale restructuring of these aggregates (e.g., from amorphous to ordered lamellar phases) upon addition of chemical redox agents that transform the oxidation state of the lipid. Our results demonstrate an approach to active and external control over both the internal nanostructures and biological behaviors of siRNA lipoplexes in complex cellular environments that could prove useful in a range of fundamental and applied contexts.

dx.doi.org/10.1021/ja403546b | *J. Am. Chem. Soc.* 2013, 135, 9111−9120

MATERIALS AND METHODS

Materials. BFDMA was synthesized using methods described previously.[27] Ascorbic acid, heparin, and lithium sulfate monohydrate were purchased from Sigma Aldrich (St. Louis, MO). Dodecyltrimethylammonium bromide (DTAB) was purchased from Acros Organics (Morris Plains, NJ). Plasmid DNA encoding firefly luciferase [pCMV-Luc, >95% supercoiled] was purchased from Elim Biopharmaceuticals, Inc. (San Francisco, CA). siRNA complementary to luciferase and green fluorescent protein (GFP) mRNA was purchased from Dharmacon, Inc. (Chicago, IL). Dulbecco's modified Eagle's medium (DMEM), Opti-MEM cell culture medium, phosphate-buffered saline (PBS), fetal bovine serum (FBS), Lipofectamine 2000, Calcein AM, Ethidium Homodimer-1, Lysotracker Red, Wheat Germ Agglutinin (WGA)-Alexa Fluor 488, and Hoechst 34580 were purchased from Invitrogen (Carlsbad, CA). Bicinchoninic acid (BCA) protein assay kits were purchased from Pierce (Rockford, IL). Glo Lysis Buffer and Steady-Glo Luciferase Assay kits were purchased from Promega Corporation (Madison, WI). Cy5 Label-IT nucleic acid labeling kits were purchased from Mirus Bio (Madison, WI). Glass inset dishes used for laser scanning confocal microscopy (LSCM) were purchased from MatTek (Ashland, MA). Deionized water (18 MΩ) was used to prepare all buffers and salt solutions. All commercial materials were used as received without further purification unless otherwise noted.

General Considerations. Electrochemical oxidation of BFDMA was performed as described previously.[29] UV−vis absorbance measurements were made using a Beckman Coulter DU520 UV−vis spectrophotometer (Fullerton, CA). Luminescence and absorbance measurements used to characterize and quantify luciferase expression, siRNA-mediated knockdown of luciferase expression, and total cell protein were performed using a PerkinElmer EnVision multilabel plate reader (luciferase: Em, 700 nm cutoff; BCA: Abs 560 nm). For LSCM experiments, siRNA was labeled using a Label-IT nucleic acid labeling kit according to the manufacturer's protocol. Labeled siRNA was purified by ethanol precipitation, and labeling densities were determined using a UV−vis spectrophotometer and methods described by the manufacturer. LSCM images were acquired using a Nikon A1R confocal microscope; images were processed using ImageJ 1.43u (National Institutes of Health; Washington, D.C.) and Photoshop CS5 (Adobe Systems; San Jose, CA). Flow cytometry analyses were performed using a BD FACSCalibur flow cytometer (BD Bioscience; San Jose, CA), and data were analyzed using the WinMDI version 2.9 software package. Student's *t*-test was used to perform statistical analyses (two different populations, $n = 6$); results were considered statistically significant for P values less than 0.05. Dynamic light scattering (DLS) experiments were conducted using a 100 mW, 532 nm laser (Coherent Compass 315M-100; Santa Clara, CA) illuminating a temperature-controlled glass cell (maintained at 25 °C) filled with a refractive-index matching fluid (decahydronaphthalene, Fisher Scientific; Pittsburgh, PA). The autocorrelation functions were obtained using a BI-9000AT digital autocorrelator (Brookhaven Instruments; Holtsville, NY).

Preparation of Lipid and Lipoplex Solutions. Reduced BFDMA solutions (1 mM) were prepared by dissolving reduced BFDMA in aqueous Li_2SO_4 (1 mM, pH 5.1). Oxidized BFDMA solutions were prepared by electrochemical oxidation of solutions of reduced BFDMA.[29] To prepare lipoplex solutions, a solution of siRNA (24 μg/mL in water) was added slowly to an aqueous Li_2SO_4 solution containing an amount of reduced or oxidized BFDMA sufficient to give the final lipid concentrations and lipid/siRNA charge ratios (CRs) reported in the text. Lipoplex solutions were incubated at room temperature for 20 min prior to use in subsequent experiments.

Characterization of siRNA-Mediated Knockdown of Luciferase Expression. COS-7 cells used in cell transfection experiments were grown in opaque polystyrene 96-well culture plates at an initial seeding density of 15×10^3 cells/well in 200 μL of growth medium (90% DMEM, 10% FBS, 100 units/mL penicillin, and 100 μg/mL streptomycin). After 24 h of incubation at 37 °C (at which point cell populations were ∼80% confluent), the medium in each well was aspirated and replaced with 200 μL of fresh growth medium and 50 μL of a mixture of Lipofectamine 2000 and plasmid DNA encoding firefly luciferase prepared according to the manufacturer's suggested protocol. After 4 h of incubation at 37 °C, culture medium was aspirated and replaced with 200 μL of fresh serum-free cell culture medium (Opti-MEM), followed by the addition of 50 μL of solutions containing lipoplexes of BFDMA and siRNA. For experiments in which ascorbic acid (AA) was added to transform lipoplexes, a 10-fold molar excess of AA was added to the culture wells via pipet immediately after the addition of the lipoplexes to cells. After 4 h of incubation at 37 °C, lipoplex-containing medium was aspirated and replaced with 200 μL of fresh serum-containing growth medium. Cells were then incubated for an additional 48 h. Luciferase expression was characterized using a luminescence-based luciferase assay kit used according to the manufacturer's protocol. Luciferase expression was normalized against total cell protein in each respective well using a commercially available BCA protein assay kit. All cell transfection experiments were conducted in replicates of six.

Characterization of Cytotoxicity of Lipoplexes. COS-7 cells were grown in clear 12-well culture plates at initial seeding densities of 15×10^4 cells/well in 200 μL of growth medium (90% DMEM, 10% FBS, 100 units/mL penicillin, and 100 μg/mL streptomycin). After 24 h of incubation at 37 °C (at which point cell populations were ∼80% confluent), the medium in each well was aspirated and replaced with 800 μL of fresh growth medium and 200 μL of a mixture of Lipofectamine 2000 and plasmid DNA encoding for firefly luciferase prepared according to the manufacturer's suggested protocol. After 4 h of incubation at 37 °C, culture medium was aspirated and replaced with 800 μL of fresh serum-free cell culture medium (Opti-MEM) followed by the addition of 200 μL of solutions containing lipoplexes of BFDMA and siRNA complementary to luciferase. For experiments in which AA was added to transform lipoplexes, a 10-fold molar excess of AA was added to the culture wells via pipet immediately after the addition of the lipoplexes to cells. After 4 h of incubation at 37 °C, lipoplex-containing medium was aspirated and replaced with 1 mL of fresh serum-containing growth medium. Cells were incubated for an additional 48 h and then analyzed for lipoplex-mediated cytotoxicity. Cells were stained with Calcein AM (a fluorescent probe used to identify live cells) and Ethidium Homodimer-1 (a fluorescent probe used to identify dead cells). Following staining, the medium was aspirated from the wells and replaced with 500 μL of trypsin with EDTA to detach the cells from the plate. The trypsin-EDTA solution was incubated with the cells for 5 min, after which the contents of each well were transferred into separate centrifuge tubes and centrifuged at 3500 rpm for 10 min. The supernatant was removed, the cell pellets were resuspended in 500 μL of PBS containing 1 mg/mL bovine serum albumin (BSA), and the tubes were centrifuged again as described above. The supernatant was again aspirated, and the cell pellets were resuspended in 500 μL of BSA-containing PBS and transferred to plastic flow cytometry tubes. The cells were kept on ice prior to characterization by flow cytometry. Fluorescence intensities corresponding to Calcein AM and Ethidium Homodimer-1 were collected along with forward- and side-scatter data for populations of 30 000 cells.

Characterization of Internalization of Lipoplexes Using LSCM. COS-7 cells were grown in glass inset confocal microscopy dishes at an initial seeding density of 2.5×10^5 cells/dish in 2 mL of growth medium. Cells were allowed to grow overnight to ∼80% confluence. Growth medium was then replaced with 2 mL of serum-free cell culture medium (Opti-MEM) and 500 μL of lipoplex solutions formulated from BFDMA and siRNA specific for luciferase (a mixture of unlabeled siRNA and 20% (w/w) of siRNA labeled with Cy-5) were added. For experiments in which AA was added to transform lipoplexes, a 10-fold molar excess of AA was added to the culture wells via pipet immediately after the addition of the lipoplexes to cells. Cells were incubated with lipoplex solutions at 37 °C for 4 h. Lipoplex solutions were aspirated, and then cells were rinsed with 50 U/mL of a heparin solution (in PBS) to promote the removal of extracellular membrane-associated lipoplexes. Cells were then stained with solutions of Hoechst 34580 (nuclear stain), Lysotracker Red (endosome/lysosome stain), and WGA-Alexa Fluor 488 (membrane

dx.doi.org/10.1021/ja403546b | J. Am. Chem. Soc. 2013, 135, 9111−9120

stain). The extent to which Cy5-labeled siRNA was internalized by cells was then characterized using LSCM. LSCM images were acquired using a 60×/1.40 NA oil immersion objective. Hoechst 34580, WGA-Alexa Fluor 488, Lysotracker Red, and Cy5-labeled siRNA were excited using laser lines at 408, 488, 561, and 638 nm, respectively. Fluorescence emission signals were collected for four individual channels and merged to create four-color images.

Characterization of the ζ Potentials of Lipoplexes. The ζ potentials of lipoplexes were characterized using a Zetasizer Nano-ZS instrument (Malvern Instruments, Worcestershire, U.K.). Lipoplexes were prepared in aqueous Li_2SO_4 solution and then diluted in Opti-MEM cell culture medium so that the final concentration of BFDMA was 10 μM. Lipid/siRNA CRs were fixed at 1.4:1 for lipoplexes of reduced BFDMA and 4.2:1 for lipoplexes of oxidized BFDMA. For experiments in which AA was added to transform lipoplexes, a 10-fold molar excess of AA was added to lipoplexes following their dilution into Opti-MEM cell culture medium. Characterization of 1 mL samples of lipoplex solutions was performed at ambient temperature using an electrical potential of 150 V. Six measurements were performed for each lipoplex solution. The Henry equation was used to calculate ζ potential from measurements of electrophoretic mobility. For these calculations, the viscosity of the lipoplex solutions was assumed to be same as that of water.

Characterization of Lipoplex Size. The average sizes of BFDMA/siRNA lipoplexes were determined by dynamic light scattering. Water and aqueous Li_2SO_4 solutions used for light scattering were filtered through a series of two 0.22 μm GV Millipore syringe filters and degassed with argon for 30 min prior to adding lipid or siRNA. Lipoplexes were prepared as described above. The scattering of light was measured at an angle of 90° with delay times ranging from 100 ns to 1−10 s. Autocorrelation functions for the intensity of the scattered light were analyzed using the CONTIN software package[37,38] to yield a distribution of aggregate sizes by assuming that the relaxation processes in solution correspond to center-of-mass diffusion.

Preparation of Lipoplexes for Characterization by Cryo-TEM. Stock solutions of BFDMA (1 mM) were prepared in 1 mM Li_2SO_4. Lipoplex solutions were prepared by adding siRNA specific for luciferase to stock solutions of BFDMA and then diluting in Opti-MEM cell culture medium. Lipoplexes formed from reduced BFDMA and siRNA were prepared at a charge ratio of 1.4:1 and contained the same molar concentrations of BFDMA as complexes formed by oxidized BFDMA and DNA at a charge ratio of 4.2:1. These charge ratios were the same as those used in cell transfection experiments, but solutions of lipoplexes used for cryo-TEM measurements were prepared at 60-fold higher overall concentrations to allow better sampling and to permit more direct comparison to the results of our past studies on cryo-TEM characterization of lipoplexes of BFDMA and plasmid DNA.

Characterization of Lipoplexes by Cryo-TEM. Specimens of lipoplexes used for characterization by cryo-TEM were prepared in a controlled environment vitrification system at 25 °C and 100% relative humidity, as previously described.[39,40] Samples were examined using a FEI T12 G^2 transmission electron microscope, operated at 120 kV, with Oxford CT-3500 or Gatan 626 cooling holders and transfer stations. Specimens were equilibrated in the microscope below −178 °C and then examined in the low-dose imaging mode to minimize electron-beam radiation damage. Images were recorded at a nominal underfocus of 1−2 μm to enhance phase contrast. Images were acquired digitally by a Gatan US1000 high-resolution (T12) cooled-CCD camera using the DigitalMicrograph software package.

RESULTS

Characterization of BFDMA-Mediated Knockdown of Luciferase Expression. We conducted a series of experiments to characterize the ability of complexes of siRNA formed using either reduced or oxidized BFDMA to knock down the expression of luciferase in transiently transfected COS-7 cells. Although our past studies demonstrate that BFDMA can be used to deliver DNA to a variety of cell types,[29−34] the studies reported here were performed using COS-7 cells for two reasons. First, because COS-7 cells are generally regarded to be easy to transfect,[41] the use of this cell line provides a robust test for the characterization of siRNA complexes that are "inactive" toward delivery (that is, our past studies demonstrate that lipoplexes of oxidized BFDMA and DNA promote very low levels of transgene expression in a cell line that is otherwise easy to transfect). Second, the majority of those past cell transfection studies using BFDMA were performed using COS-7 cells;[29−34] the use of this cell line thus provided the broadest base of data for comparison of the cell-based results of this present study. All knockdown experiments described here were performed using cells that were first transiently transfected to express luciferase using lipoplexes formed from the commercially available lipid-based agent Lipofectamine 2000 and plasmid DNA encoding firefly luciferase (see Materials and Methods for additional details).

Complexes of BFDMA and siRNA used in these experiments were formed at lipid concentrations of 6, 8, or 10 μM. These concentrations correspond to lipid/siRNA CRs ranging from 0.8:1 to 1.4:1 (for complexes of reduced BFDMA) and 2.4:1 to 4.2:1 (for complexes of oxidized BFDMA). We note here for clarity that complexes formed from reduced BFDMA and siRNA at a CR of 1.4:1, for example, contain the same molar amounts of BFDMA and siRNA as complexes formed by oxidized BFDMA and siRNA at a CR of 4.2:1 due to differences in the net charges of reduced (+1) and oxidized (+3) BFDMA (see Figure 1). The selection of the above-stated range of lipid concentrations and CRs for these initial studies was guided by the results of our past transfection studies using lipoplexes prepared using BFDMA and DNA.[30,31,33] The results of dynamic light scattering and characterization by cryo-TEM demonstrated that BFDMA and siRNA combined at these CRs form lipoplexes with sizes and structures typical of lipoplexes formed by nucleic acids and other cationic lipids (the results of those characterization studies are described in greater detail in the sections below). We used serum-free media for all of the cell-based studies reported here to permit comparison to the results of past studies on BFDMA/DNA lipoplexes and to facilitate biophysical characterization.[29−31,33,35,36]

Figure 2 shows the percent reduction of luciferase expression in COS-7 cells promoted by lipoplexes formed using BFDMA and siRNA specific for luciferase (Luc-siRNA). These results reveal that lipoplexes of reduced BFDMA (black bars) promoted high levels of gene silencing [e.g., up to ∼80%), as compared to untreated controls (striped bar)] at concentrations of BFDMA ranging from 6 to 10 μM. This level of knockdown is comparable to levels reported in several past studies using conventional cationic lipids or other lipid-like molecules to promote sequence-specific gene silencing *in vitro*.[21,24,42] Further inspection reveals that lipoplexes of oxidized BFDMA (gray bars) promoted significantly lower levels of knockdown (e.g., ∼30%) over this same range of concentrations. These results demonstrate that BFDMA can promote high levels of siRNA-mediated knockdown in cells and that the oxidation state of BFDMA plays a significant role in determining the extent to which BFDMA/siRNA lipoplexes are able to do so. These results also reveal that levels of gene silencing promoted by reduced and oxidized BFDMA do not vary significantly over this range of lipid concentrations and CRs. Past studies of DNA-based lipoplexes indicated that the cytotoxicity of reduced BFDMA increases at concentrations

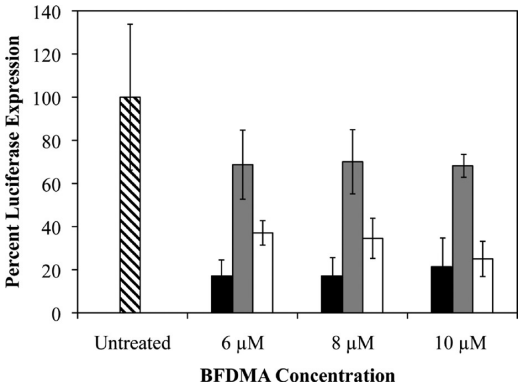

Figure 2. Percent luciferase expression in COS-7 cells 48 h after treatment with lipoplexes of reduced BFDMA and Luc-siRNA (black bars), lipoplexes of oxidized BFDMA and Luc-siRNA (gray bars), or lipoplexes of oxidized BFDMA and Luc-siRNA subsequently treated with ascorbic acid (AA, white bars). Data are shown normalized to levels of luciferase in untreated control cells (striped bar).

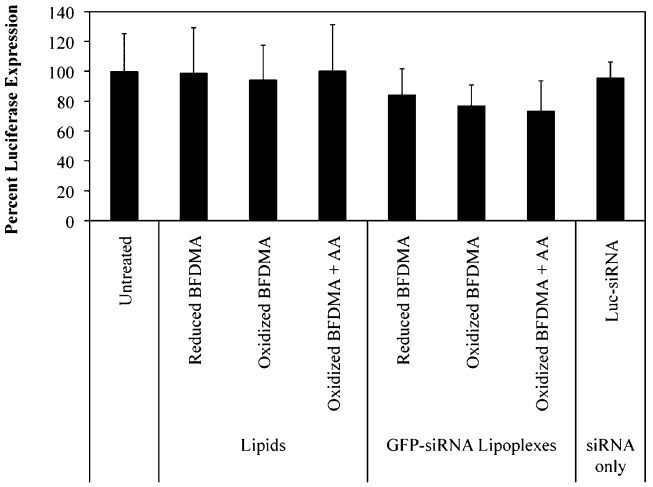

Figure 3. Percent luciferase expression in COS-7 cells 48 h after incubation in the presence of: (i) lipid only (either reduced BFDMA, oxidized BFDMA, or AA-treated samples of oxidized BFDMA at 10 μM lipid concentrations); (ii) lipoplexes of BFDMA formed using control GFP-siRNA; and (iii) samples of Luc-siRNA alone (naked siRNA). Data are shown normalized to levels of luciferase in untreated control cells.

above 10 μM;[30] lipoplexes prepared at lipid concentrations above 10 μM were therefore not investigated in this current study. The results of other experiments to characterize cytotoxicity and investigate the potential influence of other nonspecific effects that could influence the results of these studies are described in more detail below.

We demonstrated in past studies that the addition of small-molecule chemical reducing agents (such as glutathione[31] or ascorbic acid, AA[33]) to lipoplexes of oxidized BFDMA and plasmid DNA can be used to activate these otherwise "inactive" lipoplexes and promote higher levels of cell transfection. Additional results shown in Figure 2 (white bars) demonstrate that this approach can also be used as a practical means to activate lipoplexes of oxidized BFDMA and siRNA. We used AA as a reducing agent in these experiments because it reduces oxidized BFDMA rapidly[33] and because we have demonstrated that it can be used to activate DNA-based lipoplexes directly (and in the presence of cells) by simple addition of aliquots of AA to lipoplex-containing cell culture media.[33] For all experiments described here, aliquots of AA were added to BFDMA/siRNA lipoplexes after diluting them in culture media and adding them to cells (see Materials and Methods for additional details). The addition of a 10-fold molar excess of AA to lipoplexes of siRNA and oxidized BFDMA resulted in substantially lower levels of luciferase expression (white bars) compared to cells exposed to lipoplexes of oxidized BFDMA that were not treated with AA (gray bars, as discussed above) at all BFDMA concentrations and CRs tested. Levels of knockdown after the addition of AA were highest (~75%, as compared to untreated controls) at concentrations of 10 μM; under these conditions, levels of knockdown promoted by AA-treated (chemically activated) lipoplexes were similar to the levels of knockdown mediated by lipoplexes formed using reduced BFDMA (black bars). On the basis of these results, all subsequent studies were performed using formulations of lipids or lipoplexes prepared at concentrations of 10 μM BFDMA.

The results of additional control experiments and cytotoxicity screens demonstrated that the high levels of gene silencing mediated by lipoplexes of reduced BFDMA and AA-treated lipoplexes of oxidized BFDMA shown in Figure 2 are the result of sequence-specific knockdown mediated by Luc-siRNA and not a result of lipid toxicity or other nonspecific effects associated with the individual components of these lipoplexes. Figure 3 shows levels of luciferase expression in cells 48 h after incubation in the presence of: (i) lipid only (either reduced BFDMA, oxidized BFDMA, or AA-treated samples of oxidized BFDMA; all at 10 μM lipid concentrations); (ii) lipoplexes of BFDMA formed using siRNA specific for green fluorescent protein instead of luciferase (GFP-siRNA; prepared at 10 μM lipid concentrations); and (iii) samples of Luc-siRNA alone (naked siRNA).

These control experiments indicate that Luc-siRNA alone does not mediate significant levels of knockdown in the absence of BFDMA and that BFDMA alone (in both its reduced and oxidized forms) does not promote substantial nonspecific gene silencing. Treatment of cells with lipoplexes of GFP-siRNA and BFDMA (in either its reduced or oxidized forms) resulted in small reductions in average levels of luciferase expression (~20−25%) that were not statistically different from levels observed in untreated controls ($P > 0.05$). Although it is possible that small amounts of nonspecific gene silencing could occur, the levels of reduced expression observed in these experiments are also significantly lower than the levels of knockdown mediated by reduced BFDMA and AA-treated lipoplexes of Luc-siRNA shown in Figure 2 (black or white bars; reductions of ~75−80%; $P < 0.05$), suggesting that the majority of knockdown observed in those experiments was sequence specific. The results of live/dead cytotoxicity assays shown in Figure 4 demonstrate that the lipoplexes of reduced, oxidized, and AA-treated lipoplexes of BFDMA used in these experiments (prepared at a concentration of 10 μM BFDMA) are not substantially cytotoxic.

Characterization of Cellular Internalization of Lipoplexes of BFDMA and siRNA. Figure 5 shows LSCM images of COS-7 cells after 4 h of incubation in the presence of siRNA lipoplexes containing (A) reduced BFDMA, (B) oxidized BFDMA, and (C) lipoplexes of oxidized BFDMA treated with AA (all prepared at 10 μM concentrations of lipid, as described above for cell-based knockdown experiments). Cells were rinsed extensively with a heparin solution prior to imaging to promote removal of lipoplexes bound to but not internalized by

dx.doi.org/10.1021/ja403546b | J. Am. Chem. Soc. 2013, 135, 9111−9120

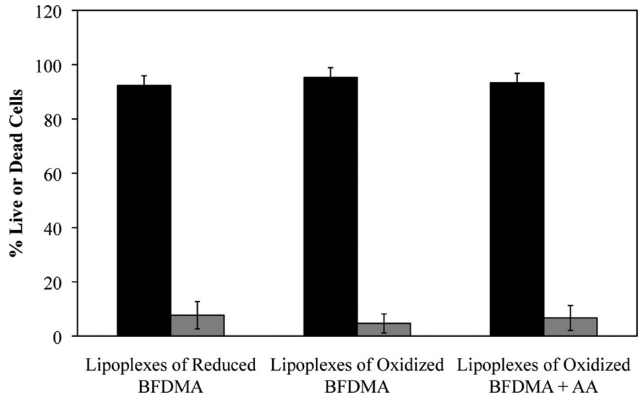

Figure 4. Percentage of live (black) and dead (gray) cells after treatment with: (i) lipoplexes of reduced BFDMA and Luc-siRNA; (ii) lipoplexes of oxidized BFDMA and Luc-siRNA; and (iii) lipoplexes of oxidized BFDMA and Luc-siRNA subsequently treated with AA. All lipoplexes were prepared at a BFDMA concentration of 10 μM (see text).

cells. In these images, fluorescence signals correspond to Cy5-labeled siRNA (red), endosome/lysosome stain (blue), cell membrane stain (green), and nuclear stain (gray).

Images of cells treated with lipoplexes of reduced BFDMA (Figure 5A) and lipoplexes of oxidized BFDMA treated with AA (Figure 5C) both reveal significant levels of internalized siRNA. Internalized siRNA was observed in two locations: (i) co-localized with endosomes and/or lysosomes (identified by white arrows; when blue signal corresponding to endosome/lysosome stain is merged with the red signal corresponding to Cy-5 labeled siRNA, magenta-colored spots are formed), and (ii) inside cells but not co-localized with endosomes or lysosomes (identified by white arrowheads). In contrast to these results, images of cells incubated with lipoplexes of oxidized BFDMA and siRNA (Figure 5B) show very low levels of internalized siRNA (examples of visible red punctate structures are again identified by white arrowheads). These results demonstrate that changes in the oxidation state of BFDMA can be used to influence or control the extent to which siRNA is internalized by cells. As discussed in greater detail below, it is through this influence on extent of internalization that the redox state of BFDMA determines the degree to which effective gene silencing can be achieved.

Physicochemical Characterization of Lipoplexes of BFDMA and siRNA. We performed additional experiments to provide insight into oxidation state-dependent differences in the physicochemical and biophysical properties of BFDMA/siRNA lipoplexes that could underlie differences in gene silencing and cellular internalization reported above. Table 1 shows the ζ potentials and average sizes of lipoplexes of reduced BFDMA, lipoplexes of oxidized BFDMA, and lipoplexes of oxidized BFDMA that were treated with AA prior to characterization. These experiments were conducted in Opti-MEM cell culture medium using lipoplexes formed at lipid concentrations and BFDMA/siRNA CRs identical to those used in the cell-based experiments described above (i.e., BFDMA/siRNA CRs of 1.4:1 and 4.2:1 for lipoplexes of reduced and oxidized BFDMA, respectively, at a 10 μM overall lipid concentration).

The average size of lipoplexes of oxidized BFDMA was measured to be ~150 nm, and the averages sizes of reduced BFDMA lipoplexes or AA-treated (chemically reduced)

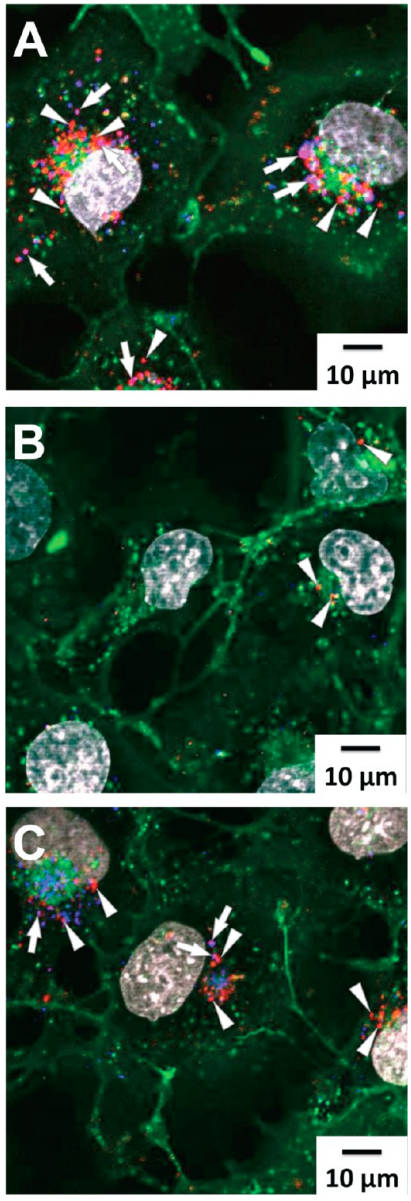

Figure 5. Representative confocal micrographs showing internalization of siRNA by COS-7 cells treated with (A) lipoplexes of reduced BFDMA and Luc-siRNA; (B) lipoplexes of oxidized BFDMA and Luc-siRNA; and (C) lipoplexes of oxidized BFDMA and Luc-siRNA subsequently treated with AA. All lipoplexes were prepared at BFDMA concentrations of 10 μM (see text). Fluorescence signals correspond to Lysotracker Red (endosome/lysosome stain; false-colored blue), WGA-Alexa Fluor 488 (membrane stain; false-colored green), Cy5-labeled siRNA (false-colored red), and Hoechst 34580 (nuclear stain; false-colored gray). Arrows point to internalized lipoplexes co-localized with endosomes and/or lysosomes (magenta color), and arrowheads point to internalized lipoplexes that are not co-localized with these vesicles.

lipoplexes of oxidized BFDMA were ~370 nm (Table 1; determined using DLS). As is typical for lipoplexes formed from cationic lipids and nucleic acids, however, the distribution of sizes in these samples was large, and the particle size distributions for these samples overlapped substantially. This polydispersity prevented the assignment of size as playing a determining role in the extent to which lipoplexes were internalized by cells. The ζ potentials of these lipoplexes were

dx.doi.org/10.1021/ja403546b | J. Am. Chem. Soc. 2013, 135, 9111−9120

Table 1. The ζ Potentials and Intensity-Average Sizes of Lipoplexes[a]

sample	ζ potential (mV)	diameter (nm)
reduced BFDMA	−7 ± 1	370 ± 270
oxidized BFDMA	−14 ± 2	150 ± 70
oxidized BFDMA + AA	−8 ± 1	370 ± 220

[a]Lipoplexes were prepared in aqueous Li_2SO_4 solution and then diluted in Opti-MEM cell culture medium so that the final concentration of BFDMA was 10 μM in all cases, and lipid/siRNA CRs were fixed at 1.4:1 for lipoplexes of reduced BFDMA and 4.2:1 for lipoplexes of oxidized BFDMA. Lipoplexes of oxidized BFDMA were treated with 10-fold molar excess of AA following their dilution into Opti-MEM cell culture medium. See text for additional details.

all negative, irrespective of the oxidation state of BFDMA or treatment with AA, but the ζ potentials of lipoplexes of oxidized BFDMA were more negative (−14 ± 2 mV) than those of lipoplexes of reduced BFDMA or AA-treated lipoplexes oxidized BFDMA (−7 ± 1 and −8 ± 1 mV, respectively).

Finally, we used cryo-TEM to characterize BFDMA/siRNA lipoplexes and determine whether changes in the oxidation state of BFDMA influence the nanostructures of these lipoplexes. These cryo-TEM analyses were performed using lipoplexes formed in serum-free cell culture medium at the same BFDMA/siRNA CRs used in the experiments described above, but at ∼60-fold higher total concentration of lipoplexes to facilitate comparisons to the results of our past cryo-TEM and small-angle neutron scattering studies on DNA-based lipoplexes (see Discussion and Materials and Methods sections for additional details).[33,36]

Figure 6A and the inset show representative cryo-TEM images of lipoplexes of siRNA and reduced BFDMA. These lipoplexes exhibited highly multilamellar spherical nanostructures. The periodicity of these multilamellar structures was 5.3 ± 0.6 nm, as determined by image analysis; this value was typical for all aggregates. Cryo-TEM characterization of lipoplexes of oxidized BFDMA and siRNA showed these samples to consist primarily of amorphous aggregates (Figure 6B and inset). Although these amorphous aggregates represented the majority of species observed during these experiments, we also occasionally observed some aggregates in these samples exhibiting partially lamellar structures (Figure 6C). In stark contrast, images of lipoplexes of oxidized BFDMA that were treated with AA prior to characterization revealed aggregates with uniformly multilamellar nanostructures (and a lamellar periodicity of 5.1 ± 0.6 nm; Figure 6D).

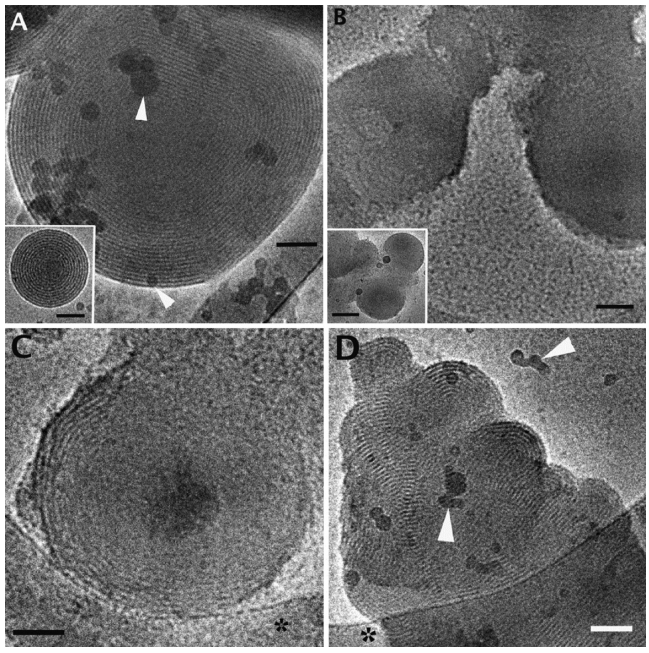

Figure 6. Cryo-TEM images of (A) lipoplexes of reduced BFDMA and siRNA, (B and C) lipoplexes of oxidized BFDMA and siRNA, and (D) lipoplexes of oxidized BFDMA and siRNA treated with AA. Asterisks and arrowheads denote the perforated carbon film used to support the lipoplexes (asterisks) and small ice crystals formed during sample preparation (arrowheads). See text for details related to preparation and analysis. All scale bars correspond to 50 nm, with the exception of the one in the inset of panel B, which corresponds to 100 nm.

DISCUSSION

The results of this study demonstrate that control over the redox state of the ferrocene groups in BFDMA can be used to exert substantial levels of control over the ability of BFDMA/siRNA lipoplexes to transport siRNA into cells and promote effective gene silencing. These observations provide a new structural and molecular basis for redox-based control over the functional behavior of siRNA lipoplexes—that is, BFDMA can be used, either alone or in combination with chemical reducing agents, to formulate siRNA lipoplexes that either (i) mediate cellular entry and promote robust gene silencing, (ii) do not promote efficient cellular entry (and, thus, do not promote effective gene silencing), or (iii) exist in a dormant or inactive state until they are "activated" by the addition of a small-molecule chemical reducing agent (achieved in this study by addition of the naturally occurring and biocompatible reducing agent AA). This redox-active lipid and the methods reported here could thus lead to the development of new approaches that permit active spatial and/or temporal control over the delivery of siRNA to cells and tissues (e.g., by the controlled delivery of reducing agents or by strategic placement of electrodes to affect the controlled or patterned electrochemical reduction of oxidized BFDMA). The ability to reversibly cycle the redox state of ferrocene under a broad range of environmental conditions,[43,44] and to use resulting differences in lipid structure to influence the biological activities of siRNA lipoplexes, renders BFDMA structurally and functionally unique among cationic lipids that have been investigated for the delivery of siRNA.

Our results reveal that the large differences in gene silencing mediated by reduced BFDMA (high levels) and oxidized BFDMA (low levels) shown in Figure 2 are primarily a consequence of the relative inability of oxidized BFDMA to promote efficient internalization of siRNA (that is, these differences in the ability of reduced or oxidized BFDMA to knock down gene expression do not appear to arise from differences in the ability of these two forms of BFDMA to mediate other downstream, intracellular processes, such as endosomal escape, etc.). The confocal microscopy images shown in Figure 5 demonstrate that lipoplexes of reduced BFDMA (Figure 5A) and "activated" (chemically reduced) lipoplexes of oxidized BFDMA treated with AA (Figure 5C) are internalized efficiently by cells, but that lipoplexes of oxidized BFDMA (Figure 5B) are not. These results are similar to those arising from confocal microscopy characterization using DNA-based lipoplexes of BFDMA.[31,33]

dx.doi.org/10.1021/ja403546b | J. Am. Chem. Soc. 2013, 135, 9111−9120

Substantial overlap in the particle size distributions for these lipoplexes as a function of the oxidation state of BFDMA (Table 1) prevent the identification of differences in size as playing a determining role in the extents of internalization discussed above, but the results of ζ potential analysis suggest that differences in surface charge are likely important. Here we note that our past studies on lipoplexes of BFDMA and plasmid DNA showed large differences in the ζ potentials of lipoplexes formed using oxidized or reduced BFDMA that correlated to the extent to which they were internalized by cells.[31,33] For example, the ζ potentials of reduced BFDMA/DNA lipoplexes were negative (approximately −17 mV) and readily entered cells; the ζ potentials of oxidized BFDMA/DNA lipoplexes were significantly more negative (approximately −34 mV) and did not enter cells efficiently.[33] Past studies suggest that the more negative ζ potentials of lipoplexes of oxidized BFDMA arise from large differences in the amphiphilicity of these two species.[35] Whereas reduced BFDMA is amphiphilic and assembles into lipoplexes with DNA through cooperative interactions that are similar to those observed for other cationic lipids, oxidized BFDMA is not amphiphilic and likely interacts with DNA in a manner more similar to that observed in complexes of other non-amphiphilic small molecules containing multiple charges (e.g., spermidine), yielding more loosely packed structures with an excess of negative charge resulting from DNA in the outer regions of the complexes.[35]

As shown in Table 1, the ζ potentials of lipoplexes of siRNA and oxidized BFDMA characterized here were also more negative (approximately −14 mV) than those of lipoplexes of reduced BFDMA (approximately −7 mV). This difference in ζ potential as a function of oxidation state is statistically significant ($P < 0.05$), but it is smaller (a difference of ∼7 mV) than that measured for DNA-based lipoplexes (a difference of ∼17 mV). The ζ potentials for the siRNA lipoplexes measured here are also both lower in magnitude than those observed for lipoplexes of plasmid DNA, likely a result of the ability of macromolecular DNA to more effectively overcompensate surface charge compared to smaller siRNA constructs. Although the overall difference in ζ potential for these siRNA complexes is smaller, these changes in ζ potential as a function of oxidation state are also consistent with differences in the extents of cellular internalization shown in Figure 5 and the resulting large differences in gene silencing shown in Figure 2. We note that the correlation observed between the relative sizes and ζ potentials of the lipoplexes of oxidized and reduced BFDMA reported here is evident in past studies of self-assembly where electrostatic interactions play an important role.[35] In general, the accumulation of excess charge inhibits growth of aggregates (i.e., the largest aggregates are observed under conditions near electroneutrality).

Our past studies demonstrated that changes in the oxidation state of BFDMA have a significant impact on the nanostructures of DNA-based lipoplexes in ways that correlate with the differences in ζ potential and ability to enter cells described above.[31,33] For example, whereas lipoplexes of plasmid DNA and reduced BFDMA possessed multilamellar nanostructures, lipoplexes of DNA and oxidized BFDMA were amorphous, as determined by small-angle neutron scattering and cryo-TEM.[33,36] It is likely that the charge of the ferrocenium groups of oxidized BFDMA disrupts the ability of this lipid to pack into lamellar nanostructures. In contrast, upon reduction of ferrocenium to ferrocene (and removal of the charges on the tails of the lipid), BFDMA is able to assume a lamellar nanostructure. A significant finding of this current study is that these substantial differences in nanostructure as a function of oxidation state of BFDMA, and their apparent biological and functional influences, are preserved and maintained in lipoplexes of BFDMA and significantly smaller siRNA constructs (Figure 6). Lipoplexes of siRNA and reduced BFDMA were highly multilamellar with a periodicity similar to that observed for lipoplexes of DNA (e.g., 5.3 ± 0.6 nm for lipoplexes of siRNA vs 5.2 ± 0.2 nm for lipoplexes of plasmid DNA),[33,36] and the majority of lipoplexes of siRNA and oxidized BFDMA were found to be amorphous. These nanostructural differences likely underlie the differences observed in the ζ potentials of siRNA-based lipoplexes, as outlined above and in our past studies on the characterization of DNA-based lipoplexes.[36] In light of past studies discussed in the Introduction[19,23−25] demonstrating that substantial differences can exist in the structures and properties of lipoplexes of plasmid DNA and siRNA, and that substantial re-optimization can be required to formulate lipoplexes of siRNA that promote high levels of gene silencing, it is significant that the range of similarities in structure, biophysical properties, biological behaviors, and redox-dependent behavior reported here using complexes of siRNA can be attained using the same BFDMA/nucleic acid charge ratios and lipoplex formulation procedures found to be most useful for the transfection of cells using plasmid DNA.

The cryo-TEM image in Figure 6D demonstrates that amorphous lipoplexes of oxidized BFDMA are transformed upon the addition of AA to lipoplexes with nanostructures that are almost completely multilamellar. This observation is consistent with the reduction of BFDMA and a subsequent and substantial physical restructuring to yield lipoplexes with nanostructures, ζ potentials, and biological activities that are otherwise similar to those of lipoplexes formed using authentic reduced BFDMA. We note that we have also observed transformations from amorphous to multilamellar nanostructures upon the addition of AA to lipoplexes of plasmid DNA and oxidized BFDMA.[33] However, that past work showed AA-induced transformations of macromolecular DNA-based lipoplexes to lead to a mixture of amorphous structures and smaller, non-spherical aggregates with more complex lamellar structures. Our current results suggest that the substantially smaller size of the siRNA constructs used here permits faster and more complete structural reorganization of lipoplexes at the nanoscale upon *in situ* chemical reduction of oxidized BFDMA.

The co-localization of siRNA with endosomes and lysosomes observed in confocal microscopy images of cells treated with lipoplexes of reduced BFDMA (Figure 5A) and lipoplexes of oxidized BFDMA treated with AA (Figure 5C) is consistent with a mechanism of cellular entry that involves endocytosis. The observation of some intracellular siRNA that is not co-localized with these vesicles suggests that BFDMA could be able to facilitate escape from these vesicles. Additional studies will be required to investigate this possibility and evaluate mechanisms of internalization and intracellular trafficking more completely. In the context of this current study, however, the observation of siRNA that is not co-localized with acidic vesicles is consistent with cytosolic delivery and the high levels of knockdown of luciferase expression using reduced BFDMA lipoplexes or "activated" (AA-treated) lipoplexes of oxidized BFDMA shown in Figure 2. The co-formulation of BFDMA/siRNA-based lipoplexes using other lipids known to facilitate endosomal escape, an approach used in past studies to optimize formulations of cationic lipids for DNA and siRNA

delivery,[16,45,46] could be used to design redox-active lipoplexes that promote even higher levels of gene silencing.

Finally, we note again that all experiments in this study were conducted using the COS-7 cell line in serum-free culture media to provide a test for the "inactivity" of lipoplexes of oxidized BFDMA (as described above) and to permit comparison to the results of biophysical and biological characterization of DNA-based lipoplexes reported in past studies.[29−34] Recent studies demonstrate that BFDMA can be used to transfect other cell types[33] and that both reduced and oxidized BFDMA can be formulated with other lipids, e.g., dioleoylphosphatidylethanolamine, to yield DNA-based lipoplexes that transfect cells in high serum [e.g., in up to 80% serum (v/v)] without degrading the redox-based 'on/off' behavior that BFDMA affords.[34] The similarities between the physical and structural properties of BFDMA/DNA and BFDMA/siRNA lipoplexes as a function of redox state—a key feature of the results reported here—suggest that this co-formulation approach could also prove useful for the design of siRNA lipoplexes that provide active, redox-based control over gene silencing in more complex biological environments (e.g., in serum-containing media or, potentially, *in vivo*).

■ SUMMARY AND CONCLUSIONS

We have demonstrated that control over the redox state of the ferrocene groups in BFDMA can be used to control the ability of lipoplexes of BFDMA and siRNA to promote gene silencing in mammalian cells. Specifically, lipoplexes of siRNA formed using reduced BFDMA lead to high levels of sequence-specific gene silencing in mammalian fibroblast cells, but lipoplexes formed using oxidized BFDMA lead to low levels of knockdown. We have also demonstrated that otherwise inactive lipoplexes of oxidized BFDMA can be activated to induce high levels of gene silencing by the addition of the small-molecule chemical reducing agent AA, demonstrating a basis for active and external control over the delivery of siRNA to cells. Our results reveal differences in the biological activities of these lipoplexes to be a consequence of the relative inability of oxidized BFDMA to promote efficient cellular internalization of siRNA, and that overall, this behavior correlates with significant differences in the nanostructures and other physical properties (e.g., the ζ potentials) of these lipoplexes as a function of the oxidation state of BFDMA.

A significant result of this study is the observation that these key structural and biophysical features, and their influences on extents of *in vitro* gene silencing, are similar in many ways to those observed for complexes formed using BFDMA and macromolecular plasmid DNA constructs—and that they can be attained and exploited without the need to manipulate lipid/siRNA charge ratios, reoptimize other aspects of nanoparticle formulation procedures, or modify cell-based treatment protocols. These findings are surprising in light of recent studies demonstrating that large differences in the physical properties of siRNA and plasmid DNA can lead to substantial differences in the structures and properties of siRNA- and DNA-based lipoplexes formed using other cationic lipids. An additional important observation arising from this study, however, is that complexes containing substantially smaller and more mobile siRNA constructs undergo more complete structural reorganization at the nanoscale when the oxidation state of BFDMA is transformed *in situ* by the addition of a chemical redox agent.

The ability to transform the oxidation state of the ferrocenyl groups of BFDMA in complex cellular environments presents opportunities to provide control over both the physical properties and biological behaviors of siRNA-based lipoplexes in ways that are not possible using conventional cationic lipids or other lipid-like materials. Active and 'on-demand' control over the properties and biological behaviors of siRNA complexes could prove useful in a variety of fundamental contexts and, with further development, in the context of emerging biomedical applications of RNAi. In addition to the approaches to chemical reduction and activation described here, future studies will address approaches to the chemical oxidation (and potential inactivation) of lipoplexes as well as methods to exert electrochemical control over the transformations of these redox-active assemblies.

■ AUTHOR INFORMATION

Corresponding Author

ishi@tx.technion.ac.il; abbott@engr.wisc.edu; dlynn@engr.wisc.edu

Notes

The authors declare no competing financial interest.

■ ACKNOWLEDGMENTS

Financial support was provided in part by the NIH (R21 EB006168 and R01 EB006820) and the NSF through CBET 0754921 and a grant to the Materials Research Science and Engineering Center (MRSEC) at the University of Wisconsin (DMR 1121288). We gratefully acknowledge S. Hata and H. Takahashi for assistance with the synthesis of BFDMA. We thank Ms. Judith Schmidt and Dr. Ellina Kesselman for the cryo-TEM work, which was performed at the Technion Electron Microscopy Laboratory for Soft Matter, with financial support from the Technion Russell Berrie Nanotechnology Institute (RBNI).

■ REFERENCES

(1) Hannon, G. J. *Nature* **2002**, *418*, 244.
(2) Dykxhoorn, D. M.; Lieberman, J. *Annu. Rev. Med.* **2005**, *56*, 401.
(3) Leung, R. K. M.; Whittaker, P. A. *Pharmacol. Ther.* **2005**, *107*, 222.
(4) Rettig, G. R.; Behlke, M. A. *Mol. Ther.* **2012**, *20*, 483.
(5) McManus, M. T.; Sharp, P. A. *Nat. Rev. Genet.* **2002**, *3*, 737.
(6) Dorsett, Y.; Tuschl, T. *Nat. Rev. Drug Discovery* **2004**, *3*, 318.
(7) Whitehead, K. A.; Langer, R.; Anderson, D. G. *Nat. Rev. Drug Discovery* **2009**, *8*, 129.
(8) Hannon, G. J.; Rossi, J. J. *Nature* **2004**, *431*, 371.
(9) de Fougerolles, A.; Vornlocher, H.-P.; Maraganore, J.; Lieberman, J. *Nat. Rev. Drug Discovery* **2007**, *6*, 443.
(10) Zhang, S.; Zhao, B.; Jiang, H.; Wang, B.; Ma, B. *J. Controlled Release* **2007**, *123*, 1.
(11) Fattal, E.; Bochota, A. *Int. J. Pharm.* **2008**, *364*, 237.
(12) Tseng, Y.-C.; Mozumdar, S.; Huang, L. *Adv. Drug Delivery Rev.* **2009**, *61*, 721.
(13) Kim, W. J.; Kim, S. W. *Pharm. Res.* **2009**, *26*, 657.
(14) Schroeder, A.; Levins, C. G.; Cortez, C.; Langer, R.; Anderson, D. G. *J. Intern. Med.* **2010**, *267*, 9.
(15) Bruno, K. *Adv. Drug Delivery Rev.* **2011**, *63*, 1210.
(16) Scholz, C.; Wagner, E. *J. Controlled Release* **2012**, *161*, 554.
(17) Foged, C. *Curr. Top. Med. Chem.* **2012**, *12*, 97.
(18) Srinivas, R.; Samanta, S.; Chaudhuri, A. *Chem. Soc. Rev.* **2009**, *38*, 3326.
(19) Desigaux, L.; Sainlos, M.; Lambert, O.; Chevre, R.; Letrou-Bonneval, E.; Vigneron, J. P.; Lehn, P.; Lehn, J. M.; Pitard, B. *Proc. Natl. Acad. Sci. U.S.A.* **2007**, *104*, 16534.

(20) Akinc, A.; Zumbuehl, A.; Goldberg, M.; Leshchiner, E. S.; Busini, V.; Hossain, N.; Bacallado, S. A.; Nguyen, D. N.; Fuller, J.; Alvarez, R.; Borodovsky, A.; Borland, T.; Constien, R.; de Fougerolles, A.; Dorkin, J. R.; Jayaprakash, K. N.; Jayaraman, M.; John, M.; Koteliansky, V.; Manoharan, M.; Nechev, L.; Qin, J.; Racie, T.; Raitcheva, D.; Rajeev, K. G.; Sah, D. W. Y.; Soutschek, J.; Toudjarska, I.; Vornlocher, H.-P.; Zimmermann, T. S.; Langer, R.; Anderson, D. G. *Nat. Biotechnol.* **2008**, *26*, 561.
(21) Love, K. T.; Mahon, K. P.; Levins, C. G.; Whitehead, K. A.; Querbes, W.; Dorkin, J. R.; Qin, J.; Cantley, W.; Qin, L. L.; Racie, T.; Frank-Kamenetsky, M.; Yip, K. N.; Alvarez, R.; Sah, D. W. Y.; de Fougerolles, A.; Fitzgerald, K.; Koteliansky, V.; Akinc, A.; Langer, R.; Anderson, D. G. *Proc. Natl. Acad. Sci. U.S.A.* **2010**, *107*, 1864.
(22) Sparks, J.; Slobodkin, G.; Matar, M.; Congo, R.; Ulkoski, D.; Rea-Ramsey, A.; Pence, C.; Rice, J.; McClure, D.; Polach, K. J.; Brunhoeber, E.; Wilkinson, L.; Wallace, K.; Anwer, K.; Fewell, J. G. *J. Controlled Release* **2012**, *158*, 269.
(23) Spagnou, S.; Miller, A. D.; Keller, M. *Biochemistry* **2004**, *43*, 13348.
(24) Bouxsein, N. F.; McAllister, C. S.; Ewert, K. K.; Samuel, C. E.; Safinya, C. R. *Biochemistry* **2007**, *46*, 4785.
(25) Zhang, X. X.; LaManna, C. M.; Kohman, R. E.; McIntosh, T. J.; Han, X.; Grinstaff, M. W. *Soft Matter* **2013**, *9*, 4472.
(26) Kakizawa, Y.; Sakai, H.; Nishiyama, K.; Abe, M.; Shoji, H.; Kondo, Y.; Yoshino, N. *Langmuir* **1996**, *12*, 921.
(27) Yoshino, N.; Shoji, H.; Kondo, Y.; Kakizawa, Y.; Sakai, H.; Abe, M. *J. Jpn. Oil Chem. Soc* **1996**, *45*, 769.
(28) Kakizawa, Y.; Sakai, H.; Yamaguchi, A.; Kondo, Y.; Yoshino, N.; Abe, M. *Langmuir* **2001**, *17*, 8044.
(29) Abbott, N. L.; Jewell, C. M.; Hays, M. E.; Kondo, Y.; Lynn, D. M. *J. Am. Chem. Soc.* **2005**, *127*, 11576.
(30) Jewell, C. M.; Hays, M. E.; Kondo, Y.; Abbott, N. L.; Lynn, D. M. *J. Controlled Release* **2006**, *112*, 129.
(31) Jewell, C. M.; Hays, M. E.; Kondo, Y.; Abbott, N. L.; Lynn, D. M. *Bioconjug. Chem.* **2008**, *19*, 2120.
(32) Golan, S.; Aytar, B. S.; Muller, J. P. E.; Kondo, Y.; Lynn, D. M.; Abbott, N. L.; Talmon, Y. *Langmuir* **2011**, *27*, 6615.
(33) Aytar, B. S.; Muller, J. P. E.; Golan, S.; Hata, S.; Takahashi, H.; Kondo, Y.; Talmon, Y.; Abbott, N. L.; Lynn, D. M. *J. Controlled Release* **2012**, *157*, 249.
(34) Muller, J. P. E.; Aytar, B. S.; Kondo, Y.; Lynn, D. M.; Abbott, N. L. *Soft Matter* **2012**, *8*, 2608.
(35) Hays, M. E.; Jewell, C. M.; Kondo, Y.; Lynn, D. M.; Abbott, N. L. *Biophys. J.* **2007**, *93*, 4414.
(36) Pizzey, C. L.; Jewell, C. M.; Hays, M. E.; Lynn, D. M.; Abbott, N. L.; Kondo, Y.; Golan, S.; Talmon, Y. *J. Phys. Chem.* **2008**, *112*, 5849.
(37) Provencher, S. W. *Comput. Phys. Commun.* **1982**, *27*, 213.
(38) Provencher, S. W. *Comput. Phys. Commun.* **1982**, *27*, 229.
(39) Bellare, J. R.; Davis, H. T.; Scriven, L. E.; Talmon, Y. *J. Electron Microsc. Tech.* **1988**, *10*, 87.
(40) Danino, D.; Bernheim-Groswasser, A.; Talmon, Y. *Colloids Surf. A: Physicochem. Eng. Asp.* **2001**, *183*, 113.
(41) van Gaal, E. V. B.; van Eijk, R.; Oosting, R. S.; Kok, R. J.; Hennink, W. E.; Crommelin, D. J. A.; Mastrobattista, E. *J. Controlled Release* **2011**, *154*, 218.
(42) Mahon, K. P.; Love, K. T.; Whitehead, K. A.; Qin, J.; Akinc, A.; Leshchiner, E.; Leshchiner, I.; Langer, R.; Anderson, D. G. *Bioconjug. Chem.* **2010**, *21*, 1448.
(43) Rosenblum, M. In *Chemistry of the Iron Group Metallocenes: Ferrocene, Ruthenocene, Osmocene. Part One*; Seyferth, D., Ed.; John Wiley and Sons, Inc.: New York, 1965, p 48.
(44) Seiwert, B.; Karst, U. *Anal. Bioanal. Chem.* **2008**, *390*, 181.
(45) Martin, B.; Sainlos, M.; Aissaoui, A.; Oudrhiri, N.; Hauchecorne, M.; Vigneron, J. P.; Lehn, J. M.; Lehn, P. *Curr. Pharm. Des.* **2005**, *11*, 375.
(46) Ma, B. C.; Zhang, S. B.; Jiang, H. M.; Zhao, B. D.; Lv, H. T. *J. Controlled Release* **2007**, *123*, 184.